***Highlights (for review)**

Understanding the need of the compression branch to characterize hyperelastic materials.

By: M Latorre, E De Rosa, FJ Montáns

Highlights:

- The compression branch is needed to characterize materials
- Using only tensile tests a physically undetermined problem is obtained
- When using only tensile tests, the several minima obtained correspond to different compression behaviors
- Using more tests than needed results in a physically overdetermined problem
- WYPIWYG procedures need both branches because the solution is exactly obtained

Understanding the need of the compression branch to characterize hyperelastic materials

Marcos Latorre[a], Erica De Rosa[b], Francisco J. Montáns[a,*]

[a] *Escuela Técnica Superior de Ingeniería Aeronáutica y del Espacio*
Universidad Politécnica de Madrid
Plaza Cardenal Cisneros, 3, 28040-Madrid, Spain
[b] *Department of Industrial Engineering - Aerospace Division*
University of Naples Federico II
Piazzale Tecchio, 80 - 80125 Naples, Italy

Abstract

Soft biological tissues are frequently modeled as hyperelastic materials. Hyperelastic behavior is typically ensured by the assumption of a stored energy function with a pre-determined shape. This function depends on some material parameters which are obtained through an optimization algorithm in order to fit experimental data from different tests. For example, when obtaining the material parameters of isotropic, incompressible models, only the extension part of a uniaxial test is frequently taken into consideration. In contrast, spline-based models do not require material parameters to exactly fit the experimental data, but need the compression branch of the curve. This is not a disadvantage because as we explain herein, to properly characterize hyperelastic materials, the compression branch of the uniaxial tests (or valid alternative tests) is also needed, in general. Then, unless we know beforehand the tendency of the compression branch, a material model should not be characterized only with tensile tests. For simplicity, here we address isotropic, incompressible materials which use the Valanis-Landel decomposition. However, the concepts are also applicable to compressible isotropic materials and are specially relevant to compressible and incompressible anisotropic materials, because in biomechanics, materials are frequently characterized only by tensile tests.

Keywords: Hyperelasticity; Biological tissues; Experimental determination; Ogden model; Sussman-Bathe model

*Corresponding author. Tel.:+34 913 366 367.
Email addresses: m.latorre.ferrus@upm.es (Marcos Latorre), eri.derosa@studenti.unina.it (Erica De Rosa), fco.montans@upm.es (Francisco J. Montáns)

1. Introduction

Soft biological tissues have a complex behavior. These materials sustain large deformations, typically behave in an anisotropic manner, have viscous effects, suffer damage and may grow or adapt (Humphrey, 2013; Fung, 2013). The basic ingredient over which formulations to model this behavior are constructed is the hyperelastic behavior. Hyperelastic behavior is a typical elastic behavior at large strains also found in rubber-like solids. The experiments of Treloar (1944) are well known to describe this type of behavior. In hyperelasticity it is assumed that there is a stored energy function. The first derivative of this stored energy function gives the stresses and the second derivative gives the tangent moduli (Ogden, 1997; Holzapfel, 2000).

The shape of the stored energy is usually assumed beforehand but some degrees of freedom are allowed through material parameters. These material parameters are computed in such a way that the predicted stresses fit some experimental data presented to the model. The computational algorithm for the material parameters is a global optimization algorithm, typically the Levenberg-Marquardt algorithm (Twizell and Ogden, 1983). The number and type of experiments presented to the model vary in the literature. In isotropic materials, sometimes only the tensile test (the extension part of the curve) is used to characterize the material and then the result is checked against other experiments (Khajehsaeid et al., 2013; Lopez-Pamies, 2010; Maeda et al., 2015; Steinmann et al., 2012; Bechir et al., 2006). In other cases, the authors analyze fittings to the tensile test curve alone on one side (or to other single curve, as in Kakavas (2000)) and with several types of experimental data together on the other side (Twizell and Ogden, 1983; Maeda et al., 2015; Gendy and Saleeb, 2000; Stumpf and Marczak, 2010). Some works use uniaxial tension curves together with equibiaxial tension curves (Pancheri and Dorfmann, 2014; Ogden et al., 2004; Palmieri et al., 2009), curves from a uniaxial tension-compression test (Bradley et al., 2001), curves from biaxial tests (Ogden et al., 2004; Ogden, 2004; Hariharaputhiran and Saravanan, 2016), curves from uniaxial tests alone and several combinations of tests simultaneously in the same work (Mansouri and Darijani, 2014), and so on. Stumpf and Marczak (2010) show that, "even if a model fits accurately with a single set of experimental data, caution should be taken when using these parameters to simulate the elastomer behavior under a different, or even a combined, case of deformation". This empirical conclusion is given in different works (Urayama, 2006), and goes back at least to the work of Treloar (1975). However, the problem has not been properly and definitely addressed because as recently mentioned in Destrade and Dorfmann (2015), "some codes even perform the curve fitting exercise for its users, who are simply required to provide experimental data from a tensile test performed on a given soft material. As it happens, non-unicity of the best-fit parameter set can occur when $N \geq 2$"(where N is the number of terms of Ogden's model). Experimental evidence shows that in some materials there is a symmetry between the tension and the compression branches, so in these cases it is possible to reformulate constitutive models as to explicitly take this fact into consideration (Moerman et al., 2016). In Ogden et al. (2004) an analysis of the goodness of the predictions obtained when using several combinations of tests is performed, concluding that the combination of both uniaxial and equibiaxial tension tests gives the best results to this question. However, no clear physical explanation for this important conclusion is given for the recommendation apart from the numerical evidence based on a particular model. Recently Puglisi and Saccomandi (2016) also conclude that "this non-uniqueness can represent a limitation of the theory both in the perspective of a physical interpretation of these parameters and in the numerical applications. In particular, two distinct sets of parameters giving an equally good fitting in tension lead to completely different predictions for other deformations, see Ogden et al. (2004) for an example ". Again, no clear explanation is given for the addressed problem; the authors just refer to the numerical evidence. From the foregoing works, it is obvious that a well-informed researcher, specially since the work of Ogden et al. (2004), knows that more than a tensile test is needed to characterize a hyperelastic material and that in isotropy tensile and equibiaxial tests are a good combination. This is a very important (frequently overlooked) conclusion because as mentioned in Ogden et al. (2004) "careful mathematical analysis is needed to ensure confidence in the resulting numerical solutions". However, what is lacking in the literature is precisely a proper explanation and understanding of the underlying physical reason which clearly states the tests needed to adequately characterize the material, so the desired confidence in numerical solutions is obtained.

In anisotropic hyperelastic materials, specially in biological tissues, the same situation is encountered. Because these materials are more complex and experimental curves more difficult to obtain, it is frequent to use only extension data to characterize or study the material, i.e. to obtain the material parameters, see for example Holzapfel (2006); Li and Robertson (2009); Shearer (2015); Holzapfel et al. (2015); Itskov and Aksel (2004); Grytz et al. (2016); Angeli et al. (2015); Chen et al. (2016); Pierce et al. (2015), among many others. These parameters from tensile tests have also been used to perform simulations on biaxial experiments and compare to experimental data (Cooney et al., 2015). Sometimes planar tension tests alone (Santamaría et al., 2015) or biaxial, equibiaxial or tensile membrane tests alone are also used, see for example Sacks (2003); Natali et al. (2006); Tricerri et al. (2016);

Cortes and Elliott (2016); Gasser (2016); Kamenskiy et al. (2015); Lee et al. (2016); Fehervary et al. (2016), just to name some recent works. Compression tests are also used to characterize anisotropic materials, see for example Chen et al. (2015); Van Loocke et al. (2006); Ateshian et al. (1997). In summary, it seems to be unclear in the literature which is the number of tests needed to adequately determine the material behavior because the underlying physical reason was probably not well understood even in the isotropic model. This problem is specially significative in biomechanics, where the material parameters of a large number of models are determined using only one type of test, for example tensile tests in one or two directions. Then, the material constants determined this way are thereafter used to predict the behavior in other tests or used in general finite element simulations expecting that the material behavior is represented in any loading condition that may appear at the stress integration points.

What-you-prescribe-is-what-you-get (WYPIWYG) hyperelasticity (or spline-based hyperelasticity) is a different approach. The incompressible isotropic model, which is based on the Kearsley and Zapas (1980) inversion formula, is due to Sussman and Bathe (2009) and is currently available in the general-purpose commercial finite element code ADINA. The transversely-isotropic and orthotropic incompressible versions, which employ a more general inversion formula, are due to Latorre and Montáns (2013, 2014). These models present a purely phenomenological and mainly numerical approximation to the problem. Stored energy shapes are not given beforehand, but obtained from the experimental data. The stored energy is exactly obtained, up to machine precision (Latorre et al., 2016; Romero et al., 2017), in as many points as desired, and then it is interpolated using splines (although other interpolation functions are possible).

However, the WYPIWYG approach needs *both* the extension *and* the compression part of the uniaxial curves. In this approach it is not possible to obtain the stored energy without the explicit knowledge of both extension and compression branches. As in the infinitesimal framework, in general, a correct complete set of tests must be specified to determine the material behavior in both isotropic and anisotropic WYPIWYG procedures (Sussman and Bathe, 2009; Latorre and Montáns, 2013, 2014; Latorre et al., 2016; Romero et al., 2017). If one is not known, a reasonable assumption must be made. This could be considered as a disadvantage of WYPIWYG models when compared to analytical ones determined from optimization procedures. However, we explain here the reason why both extension and compression parts are always needed to correctly (and completely) define not only WYPIWYG models, but most models as well. Then, the goodness of the material parameters to fit the extension part of the tensile test alone says little, in general, about the goodness of those material parameters to represent the overall material behavior. As with the WYPIWYG models, if one branch is not known, a reasonable hypothesis should be made before computing the material parameters *over all, experimental and assumed, data.* This way the model will behave as the modeler expects and confidence in numerical solutions is obtained.

The concepts explained in this paper are general and applicable to any material, compressible or incompressible, isotropic or anisotropic, and to any stored energy function. However, they are easily explained for isotropic incompressible materials employing the Valanis-Landel hypothesis (Valanis and Landel, 1967) because only one curve (including extension and compression parts) is involved and the exposition is simpler.

The rest of the manuscript is structured as follows. We first address the usual form of determining the material parameters in traditional phenomenological models. Then we address the inversion formula that solves exactly the problem of finding the stored energy density values from experimental data, and the Sussman-Bathe interpolating procedure to obtain an analytical function. We highlight the need of the compression branch in applying that formula, and the completeness of the tension and compression branches to fully determine the material behavior in any loading condition. Finally we address some examples considered in Ogden et al. (2004) using Ogden's model in order to analyze the conclusions raised therein from a new perspective. We finally show that the stored energy functions obtained following the proposed procedure may be employed with confidence if the constitutive hypotheses hold.

2. The usual approach for determining stored energy functions

In order to guarantee the absence of dissipation in hyperelastic material models, the common approach consists of assuming the existence of a strain energy function with a specific analytical shape (e.g. exponential, logarithmic, etc.). The initial function depends on some freely prescribed material parameters which are unknown beforehand. These material parameters are obtained from a numerical optimization algorithm in such a way that the analytical predictions for the experimental test(s) are as close as possible (in a least squares sense) to the experimental observations for the given test(s), hence determining the actual, final expression for the material model at hand. A commonly used optimization algorithm is the Levenberg–Marquardt algorithm (Twizell and Ogden, 1983). Hereafter, and for the matter of simplicity along the exposition, we assume that the material being characterized is isotropic and incompressible.

An example of error function (objective function) to be employed in the minimization problem is given in Ogden et al. (2004) as

$$S(\boldsymbol{\beta}) := \left\| \boldsymbol{\tau}(\hat{\boldsymbol{\lambda}}, \boldsymbol{\beta}) - \hat{\boldsymbol{\tau}} \right\|^2 = \sum_{n=1}^{N} [\tau(\hat{\lambda}_n, \boldsymbol{\beta}) - \hat{\tau}_n]^2 \tag{1}$$

where $\hat{\boldsymbol{\lambda}} = [\hat{\lambda}_1, \hat{\lambda}_2, ...\hat{\lambda}_N]^T$ is the vector of the N experimental stretches associated to the corresponding N experimental Kirchhoff stresses $\hat{\boldsymbol{\tau}} = [\hat{\tau}_1, \hat{\tau}_2, ...\hat{\tau}_N]^T$, $\tau(\hat{\lambda}_n, \boldsymbol{\beta})$ are the stresses predicted by the analytical model at the discrete experimental stretch values $\hat{\lambda}_n$ and $\boldsymbol{\beta} = [\beta_1, .., \beta_{\bar{M}}]$ are the selected $\bar{M}$ model parameters (i.e. design variables of the optimization procedure). The norm $\|\cdot\|$ is the standard 2-norm. Note that the hat accent implies experimental discrete values, whereas the absence of the accent implies values obtained from the assumed continuum analytical model. Then, the problem is to find the set of material parameters $\boldsymbol{\beta}$ that minimizes the error function, i.e.

$$\boldsymbol{\beta} = \arg \left(\min_{\boldsymbol{\beta}} S(\boldsymbol{\beta}) \right) \tag{2}$$

We note that the principal Kirchhoff stresses $\boldsymbol{\tau}$ (coincident to Cauchy stresses $\boldsymbol{\sigma}$ by incompressibility) may be obtained from the assumed stored energy function $\mathcal{W}$ as

$$\tau_i = \lambda_i \frac{\partial \mathcal{W}}{\partial \lambda_i} + p \quad \text{with } i = 1, 2, 3 \tag{3}$$

where p is the Lagrange multiplier associated with the incompressibility constraint and $\mathcal{W}$ is a function of the stretches for a given material, but a function also of the material parameters $\boldsymbol{\beta}$ when considering different materials (i.e. different fits). The principal first Piola–Kirchhoff (and nominal) stresses are obtained by

$$P_i \equiv \frac{\tau_i}{\lambda_i} = \frac{\partial \mathcal{W}}{\partial \lambda_i} + \frac{p}{\lambda_i} \quad \text{with } i = 1, 2, 3 \tag{4}$$

It should be obvious from Eqs. (3) and (4) that minimizing the experimental error in Kirchhoff stresses is not the same as minimizing it in first Piola–Kirchhoff stresses unless the error completely vanishes; this last situation being obtained within the spline-based interpolation procedures (Sussman and Bathe, 2009; Latorre and Montáns, 2013, 2014; Latorre et al., 2016; Romero et al., 2017). However, we address here only the typical error function given in Ogden et al. (2004).

In particular, Ogden's model for isochoric isotropic materials, as given in Ogden et al.

(2004), assumes exponentiated shapes of the form

$$\mathcal{W} = \sum_{m=1}^{M} \frac{\mu_m}{\alpha_m} \left(\lambda_1^{\alpha_m} + \lambda_2^{\alpha_m} + \lambda_3^{\alpha_m} - 3\right) \tag{5}$$

where $\lambda_1, \lambda_2, \lambda_3$ are the principal stretches of the deformation, constrained by $\lambda_1 \lambda_2 \lambda_3 = 1$. The model is based on the Valanis–Landel decomposition. For practical purposes the sum in Eq. (5) must be restricted to a limited number of $\bar{M} = 2M$ parameters, typically six ($M = 3$) to eight ($M = 4$) (Ogden, 1997; Ogden et al., 2004) —more terms may be required in some cases (Sussman and Bathe, 2009).

According to the common approach, to fully determine the strain energy function $\mathcal{W}$, we have to obtain the set of parameters $\boldsymbol{\beta} = [\alpha_1, .., \alpha_M, \mu_1, .., \mu_M]$ such that the derived stresses better adjust to experimental data. The relevant issue in the present paper is to show that some widely used procedures are ill-posed from a physical standpoint, which clearly explains why the obtained results strongly affect the predictions under loadings different from those used to determine the strain energy function.

Ogden et al. (2004) consider several possible procedures in order to determine the parameter set $\boldsymbol{\beta}$. According to Ogden et al. (2004), the experimental stress data $\hat{\boldsymbol{\tau}}$ used to find the material parameters can be obtained by one of the following procedures:

- By a uniaxial tension experiment alone
- By an equibiaxial tension experiment alone
- Simultaneously by both uniaxial and equibiaxial tension experiments

In their work Ogden et al. (2004) show that these three different cases lead to different sets of parameters. Moreover, they show that even if a single type of the three experimental possible procedures to determine the material parameters is considered, but the optimization fitting process is initialized with different starting values, then different parameter sets are obtained. From a mathematical standpoint, this implies that the problem presents several local minima and that there is no guarantee of reaching a global minimum. This procedure just gives a numerically better fit of the model to the specific experimental data presented according to the selected objective function. In summary, for Ogden's model (the situation is similar in most models), the minimum of the optimization problem depends on:

- The number of terms considered in Eq. (5)

- The type of the experimental data used in the problem
- The (arbitrary) initial values given to the model parameters
- The selected objective function to be optimized
- The number of experimentally measured points

Then, the question raised is whether the material model obtained this way (the obtained material parameters) represents the material behavior in any other loading situation, and whether it does better than any other possible solution (any other possible minimum) so the required confidence in numerical solutions is obtained. In an attempt to solve this issue, the recommendation in Ogden et al. (2004) was to use more than a set of experimental data, possibly of different test types. However, the underlying reason for that recommendation is not given, maybe because the solution to this very delicate question is hidden by the global nature of the parameter fitting procedure. Following a very different approach we explain below in the large strain context, both physically and mathematically, the underlying reason for the multiplicity of solutions reported in Ogden et al. (2004).

3. The generalized inversion formula and the Sussman–Bathe procedure

The procedure in Sussman and Bathe (2009) is essentially different (in both conceptual and numerical terms) to the typical approach employed in hyperelasticity. Instead of assuming the shape of the stored energy function and performing a global parameter fitting procedure, spline-based energy functions are used to achieve a local, exact fit of experimental data. We have extended the method to transversely isotropic materials (Latorre and Montáns, 2013) and orthotropic ones (Latorre and Montáns, 2014), in order to use them to model biological tissues as arterial wall (Latorre et al., 2016) and skin (Romero et al., 2017). The model of Sussman and Bathe, as many other isotropic models (among them Ogden's model), hinges on the Valanis and Landel (1967) decomposition of the deviatoric stored energy function, which may be written in terms of the principal isochoric logarithmic strains $E_i = \ln(\lambda_i)$, $i \in \{1, 2, 3\}$, as

$$\mathcal{W}(E_1, E_2, E_3) = \omega(E_1) + \omega(E_2) + \omega(E_3) \tag{6}$$

where $\omega(E)$ stands for the same scalar-valued function of each principal logarithmic strain component E_i. These strains are subjected to the incompressibility condition which is written as in the infinitesimal case: $E_1 + E_2 + E_3 = 0$. Then, in order to determine the single-variable function $\omega(E)$, a tension-compression test data set $\hat{\boldsymbol{\sigma}}_u(\hat{\boldsymbol{E}}_1)$ is needed. In the case of analytical (assumed) models, as for the case of Ogden's model, the shape of $\omega(E)$ is given beforehand. In clear contrast, in the procedure promoted by Sussman and Bathe, the solution function $\omega(E)$ is exactly computed at as many points as desired and then the analytical expression is built through spline interpolations, hence any shape of $\omega(E)$ (e.g. exponential, polynomial, etc.) may be captured. In order to do so, Sussman and Bathe (2009) employed the Kearsley and Zapas (1980) formula, which was compacted and generalized for anisotropy in Latorre and Montáns (2013).

The Kearsley and Zapas (1980) formula solves the equilibrium equation of the (tension-compression) uniaxial test for the case of incompressible isotropic hyperelasticity. In this case, the governing equation is —we denote by $\sigma_u \equiv \sigma_1$ the stresses in the uniaxial test direction

$$\sigma_u(E_1) = \omega'(E_1) - \omega'(E_2(E_1)) = \omega'(E_1) - \omega'\left(-\tfrac{1}{2}E_1\right) \tag{7}$$

where the last addend is due to the initially unknown pressure, which in this test is determined by the stress-free condition in both transverse directions, specifically $\sigma_2 = \sigma_3 = 0$. Note that as in the infinitesimal case $E_2(E_1) = E_3(E_1) = -E_1/2$. We here remark that Eq. (7) is valid in general (not just for a specific model), as long as the Valanis-Landel hypothesis is assumed. We also remark that this equation clearly shows that the stresses in a tensile test depend (also) on the compression branch of the stored energy. In order to solve Eq. $(7)_1$ for $\omega'(E)$, consider the following recursive expressions

$$\sigma_u(E_1) = \omega'(E_1) - \omega'(E_2(E_1)) \tag{8}$$

$$\sigma_u(E_2(E_1)) = \omega'(E_2(E_1)) - \omega'\left(E_2^{(2)}(E_1)\right) \tag{9}$$

$$\dots$$

$$\sigma_u\left(E_2^{(k)}(E_1)\right) = \omega'\left(E_2^{(k)}(E_1)\right) - \omega'\left(E_2^{(k+1)}(E_1)\right) \tag{10}$$

$$\dots$$

where we defined

$$E_2^{(k)}(E_1) := \underbrace{E_2(E_2(\dots E_2(E_1)))}_{k\ \text{times}} \tag{11}$$

with

$$E_2^{(0)}(E_1) := E_1 \tag{12}$$

Adding all equations we obtain *the generalized inversion formula* for the uniaxial test

$$\omega'\left(E_1\right)=\sum_{k=0}^{\infty}\sigma_u\left(E_2^{(k)}\left(E_1\right)\right) \tag{13}$$

where we have used the fact that $E_2^{(\infty)}\left(E_1\right)=(-1/2)^{\infty}E_1=0$ and we take $\omega'\left(0\right)=0$. Since $\sigma_u\left(0\right)=0$, this solution series converges to any required precision in a finite number of terms. For the isotropic case at hand the inversion formula Eq. (13) is the same as the Kearsley and Zapas formula (in compact form), which may be written as

$$\omega'(E_1)=\sum_{k=0}^{K}\sigma_u\left(\left(-\frac{1}{2}\right)^k E_1\right) \tag{14}$$

$$=\sigma_u\left(E_1\right)+\sigma_u\left(-\frac{1}{2}E_1\right)+... \tag{15}$$

We note that for $K\to\infty$ the solution is analytically *exact* for each value E_1, either positive (tension branch) or negative (compression branch), and for K sufficiently large (typically 20 to 30) the solution is exact to machine precision. We here remark that Eq. (14) is the general solution of the derivative of the stored energy function density for incompressible isotropic materials fulfilling the Valanis-Landel decomposition, *not the solution of any particular model.*

Then, the solution of Eq. (14) needs the evaluation of a stress-strain curve $\sigma_u\left(E\right)$ at different points for each given value $\hat{E}_1$, more precisely at $\left(-\frac{1}{2}\right)^k\hat{E}_1$ with $k=1,...,K$, which do not necessarily coincide with values contained within the experimental points set $\hat{\boldsymbol{E}}_{\mathbf{1}}$ (where the set $\hat{\boldsymbol{\sigma}}_u$ is known). Therefore, the N experimental data points $\hat{\boldsymbol{\sigma}}_u(\hat{\boldsymbol{E}}_1)$ are initially interpolated using piecewise cubic splines in order to be able to evaluate $\sigma_u\left(E\right)$ in the right-hand side of Eq. (14) at any arbitrary argument value E. Then, Eq. (14) is evaluated at a new set of equispaced values $\bar{\boldsymbol{E}}_1$, say $\bar{\boldsymbol{\omega}}'\left(\bar{\boldsymbol{E}}_1\right)$. Note that $\bar{\boldsymbol{E}}_1\neq\hat{\boldsymbol{E}}_1$ in general. In order to have an analytical function that may be employed in any loading situation for both analytical calculations and finite element analyses, the computed points $\bar{\boldsymbol{\omega}}'\left(\bar{\boldsymbol{E}}_1\right)$ are finally interpolated to give as a result the actual spline function $\omega'\left(E\right)$, which is a continuous analytical function with also continuous first (i.e. $\omega''\left(E\right)$) and second (i.e. $\omega'''\left(E\right)$) derivatives.

4. The necessity of the compression branch in hyperelastic tension tests

The inversion formula Eq. (14), which solves Eq. (7) up to the desired precision, clearly shows that in order to obtain a stored energy (first derivative) function value $\bar{\omega}' = \omega'\left(\bar{E}_1\right)$ for a given strain value $\bar{E}_1 > 0$ of the tension branch, we need to know not only the stress value $\sigma_u\left(\bar{E}_1\right) > 0$, but also the stress values at $E_2^{(k)}\left(\bar{E}_1\right) = (-1/2)^k \bar{E}_1$, which *take both tension (positive, i.e. k is even) and compression (negative, i.e. k is odd) values of the curve $\sigma_u(E)$*. Analogously, we need both tension and compression branches of $\sigma_u(E)$ in order to compute any stored energy (first derivative) function value $\bar{\omega}' = \omega'\left(\bar{E}_1\right)$ with $\bar{E}_1 < 0$. Therefore it is mathematically apparent that in general we need both the tension *and* the compression branches of the uniaxial stress-strain curve $\sigma_u(E)$ to determine the stored energy function. Note that if the complete tension-compression curve $\sigma_u(E)$ is known from experiments, then the solution curve $\omega'(E)$ is exact and unique, i.e. the solution to the strain energy determination problem. Because of its uniqueness, this energy will exactly predict the material behavior in any other deformation state if the constitutive hypotheses (isotropy, Valanis-Landel, etc.) are correct.

This conclusion should also be clear from a physical point of view when considering the incompressibility constraint in the uniaxial test, which imposes conditions on the opposite branch of $\omega(E)$ through the Lagrange multiplier, note that the second addend in the right-hand side of Eq. (7) is evaluated at a compression (tension) strain value for $E_1 > 0$ ($E_1 < 0$).

These arguments explain some of the correct conclusions given in Ogden et al. (2004), which are raised therein from a purely numerical perspective. In Ogden et al. (2004) it is shown that when both uniaxial and equibiaxial tension data are used simultaneously to find the parameters of the Ogden stored energy function, then the values of the solution parameters remain the same. This holds even when varying the starting values of the parameters chosen to initialize the optimization fitting process (see Section 4.4 of Ogden et al. (2004)). However, we want to remark herein that this result is not a consequence of just considering more tests (not only one) or more distinct type of tests (not only uniaxial), as it may be inferred from that Reference. The obtained results are a consequence of considering in this case a proper set of experimental data needed to determine both the tension *and* the compression branches of the Valanis–Landel term ω of the Ogden stored energy function, as we show next. The use of a tensile test and an equibiaxial test was described in Ogden et al. (2004) as a good option based on their numerical evidence. However, since this model fits the experimental measurements in a least squares sense, note that even in this case there is no guarantee that the solution of the optimization procedure is unique because in general the objective function is not globally convex in its arguments. However the solutions obtained this way will yield similar predictions in any loading situation.

In order to show that the procedure followed in Section 4.4 of Ogden et al. (2004)

is consistent with the model hypotheses, we just note that, as it is well-known, the compression branch of a uniaxial test is indirectly given by the tension part of the corresponding equibiaxial test, see for example Rivlin and Saunders (1951); Barenblatt and Joseph (2013); Treloar (1975). For Valanis-Landel materials, the governing equation of the equibiaxial test becomes

$$\sigma_e\left(E_1\right) = \omega'\left(E_1\right) - \omega'\left(-2E_1\right) \tag{16}$$

where σ_e is the equibiaxial stress. Comparing the governing equation of the uniaxial tension test, Eq. (7), to that of the equibiaxial test, Eq. (16), we obtain the equivalence relation

$$\sigma_u\left(-2E\right) = -\sigma_e\left(E\right) \tag{17}$$

which clearly shows that an "experimental" uniaxial compression curve, $\sigma_u\left(-2E < 0\right) < 0$, may be obtained from the truly experimental equibiaxial tension curve, $\sigma_e\left(E > 0\right) > 0$ (Rivlin and Saunders, 1951). Indeed, it can be easily shown using recursive expressions that the equibiaxial test Eq. (16) may also be solved by the following *generalized inversion formula* for the equibiaxial test

$$\omega'\left(E_1\right) = -\sum_{k=0}^{\infty} \sigma_e\left(\left(-\frac{1}{2}\right)^{k+1} E_1\right) \tag{18}$$

which, upon the consideration of Eq. (17) in every term of the series, exactly converts to the generalized inversion formula for the uniaxial test, Equation (13).

As a summary, a physically well-posed procedure to determine a hyperelastic isotropic incompressible material model based on the Valanis–Landel hypothesis needs experimental stress-strain data from, for example:

- A uniaxial test performed under both tension and compression, or
- A uniaxial test performed under tension and an equibiaxial test performed under tension, or
- An equibiaxial test performed under both tension and compression.

In the first case we would directly obtain the whole experimental curve $\sigma_u\left(E\right)$, see Bradley et al. (2001). In the second and third cases, we can apply the equivalence of Eq. (17) to the respective equibiaxial test branches in order to obtain the equivalent whole curve $\sigma_u\left(E\right)$. Then, the strain energy function term $\omega\left(E\right)$ is properly determined from the equivalent "experimental" curve $\sigma_u\left(E\right)$, either following the parameter fitting, least-squares-based approach or the exact, spline-based procedure. Note that if we follow the usual approach, the conversion from equibiaxial data to the corresponding uniaxial data is not strictly necessary. This last case is the one addressed in Section 4.4 of Ogden et al. (2004), where the Ogden model is used to simultaneously fit both uniaxial and equibiaxial tension tests, see also Pancheri and Dorfmann (2014); Palmieri et al. (2009).

Finally, we note that in the foregoing comments we assumed that a relation between the tension and the compression branches is unknown beforehand. For example, if symmetry may be assumed (Moerman et al., 2016), then $\omega(-E) = \omega(E)$ and one branch is sufficient because the complete tension-compression data can be obtained from it. Other exception are models which implicitly establish a relation between the tension and the compression branches, as for example the Gent chain model analyzed also in Ogden et al. (2004). However, that relation may be valid only for specific materials and should be verified accordingly for other materials. Furthermore, in models which do not follow the Valanis-Landel decomposition (as the mentioned Gent model), the coupling between principal strain components should be verified with additional tests because the stretch in a second direction changes the uniaxial tension-compression curve (Marckmann and Verron, 2006).

5. Examples

5.1. Predictions using the Ogden model

In this section we compute the uniaxial tension-compression stress predictions given by the Ogden model when the set of parameters given in Sections 4.1, 4.3 and 4.4 of Ogden et al. (2004) are employed. The predictions are then compared with the experimental data reported by Treloar (1944).

In Figure 1.*a* we represent the equivalent uniaxial tension-compression experimental data of Treloar (1944). The uniaxial tension points $\hat{\sigma}_u(\hat{E}_u > 0) > 0$ in Figure 1.*a* are directly represented from the actual uniaxial tension test. The compression points $\hat{\sigma}_u(\hat{E}_u < 0) < 0$ are obtained from the actual equibiaxial tension test points $\hat{\sigma}_e(\hat{E}_e > 0) > 0$ through the transformations $\hat{E}_u = -2\hat{E}_e < 0$ and $\hat{\sigma}_u = -\hat{\sigma}_e < 0$, recall Eq. (17). In the following, we will make use of these experimental data points in order to explain all the differences encountered among the different possibilities being addressed.

Consider first the case in which the Ogden model parameters are obtained employing only the tension experimental data of the uniaxial test in the optimization procedure, i.e. the material parameters reported in Section 4.1 of Ogden et al. (2004). We represent in Figure 1.*a* the uniaxial tension-compression stress predictions given by the Ogden model with the parameter sets OT, OSS_1, OSS_2 and OSS_3 of Table 1 in Ogden et al. (2004), for which $M = 3$. It is clearly seen in that Figure that the stress-strain behavior under tension loading is accurately predicted by the model in all the presented cases. However, it can also be observed in that Figure that the compression branch associated to each material parameter set becomes very different to each other and a consequence of the arbitrary starting set, instead of being defined from the actual material behavior. A similar issue arises regarding both transverse strains (Latorre et al., 2016) and material-symmetries congruency (Latorre and Montáns, 2015) in biological tissues.

In Figure 1.b we represent the first derivative function of the Valanis–Landel–type term $\omega(E)$ for the different solution sets OT, OSS_1, OSS_2 and OSS_3 given in Table 1 of Ogden et al. (2004). Remarkably, very different solution functions are obtained in each case within *both* the tension and the compression domains of $\omega(E)$. The solution is far from being unique and far from having a clear tendency. As explained, the results in this figure bring another important conclusion, i.e. that the goodness of the fit of the tension branch says little about the goodness of the computed stored energy function, in general, so confidence in subsequent numerical predictions cannot be obtained. Indeed, the parameter sets OSS_1 and OSS_2 give very low, and similar, relative errors associated to the uniaxial tension test fit (see Figure 2 in Ref. Ogden et al. (2004)), but the respective terms $\omega(E)$ are very different, *even for* $E > 0$ (see Figure 1.b).

We represent in Figure 2 the results obtained using the Ogden model with the parameter sets OT, OSS_1, OSS_2 and OSS_3 given in Table 2 of Ogden et al. (2004), for which $M = 4$. Again, the predictions of the compression branch are model-dependent (consequence of the arbitrary starting values, see Figure 2.a) and the respective strain energy functions are very different to each other in the whole domain of deformations (i.e. not only in the compression domain, see Figure 2.b).

Due to the very large differences observed in the functions $\omega'(E)$ in Figures 1.b and 2.b, the differences in the predictions for a generic multiaxial loading situation will also be large if we use one set or another of those reported in Sections 4.1 of Ogden et al. (2004). We conclude that uniaxial tension data alone should never be used to determine an incompressible, isotropic hyperelastic model at finite strains (cf. Kakavas (2000)), unless the equibiaxial tension predictions (equivalently, uniaxial compression predictions) are verified against experiments subsequently (Khajehsaeid et al., 2013; Lopez-Pamies, 2010; Maeda et al., 2015; Steinmann et al., 2012; Bechir et al., 2006).

Consider now the case in which the Ogden model parameters are obtained employing only the tension experimental data of the equibiaxial test in the optimiza-

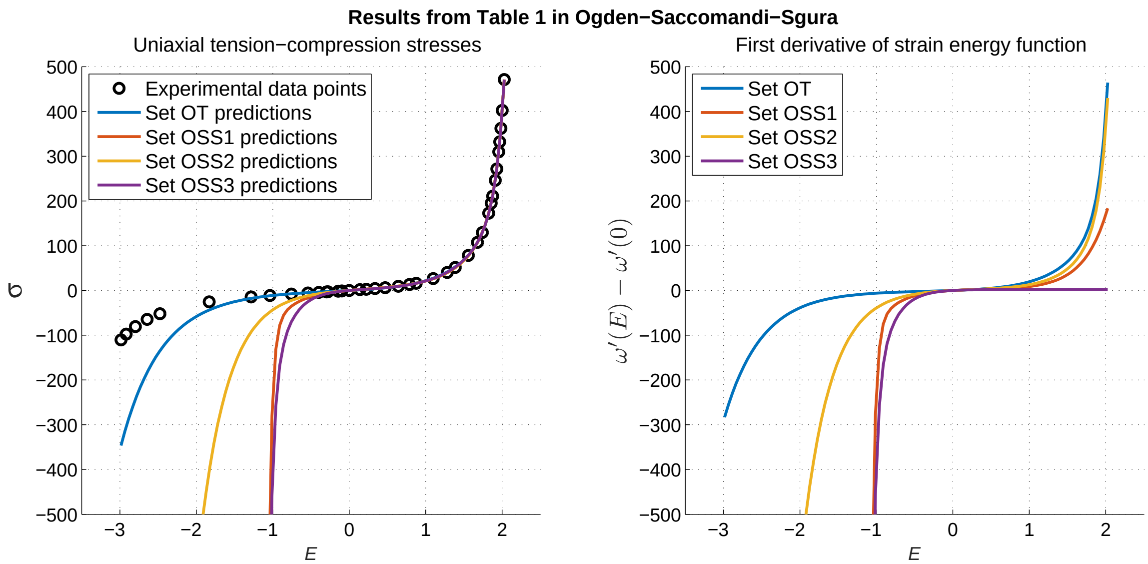

Figure 1: Left (a): Uniaxial tension-compression Cauchy stress predictions (kg / cm^2) computed by Ogden's model with $M = 3$ using parameter sets obtained by fitting uniaxial tension experimental data. Right (b): First derivative of the Ogden function term $\omega(E)$. Different curves correspond to the different parameter sets reported in Table 1 of Ogden et al. (2004).

tion procedure, i.e. the material parameters reported in Section 4.3 of Reference Ogden et al. (2004). We represent in Figure 3.a the uniaxial tension-compression stress predictions given by the Ogden model along with the parameters sets OSS_1, OSS_2 and OSS_3 of Table 3 in Ogden et al. (2004), for which $M = 3$. It is seen that the model reproduces well the equivalent uniaxial compression data points (i.e. the equibiaxial tension measurements), but the uniaxial tension predictions are arbitrary and extremely poor when compared to Treloar's data. As mentioned, the reason for the discrepancies is simply that the stored energy is not correctly determined because an important part of the information on the material behavior has been initially disregarded, so the stored energy is physically undetermined, regardless of the optimization algorithm employed and of the obtained relative errors. However, once again, the global nature of the parameter fitting procedure allows for the determination of different mathematical solutions (local minima), see Figure 3.b.

We represent in Figure 4 the results obtained using the Ogden model with the parameters sets OT, OSS_1, OSS_2 and OSS_3 of Table 4 in Ogden et al. (2004), for which $M = 4$. Again, the predictions of the equivalent compression stresses are accurate but the predictions of the tension branch are arbitrary (see Figure 4.a), instead

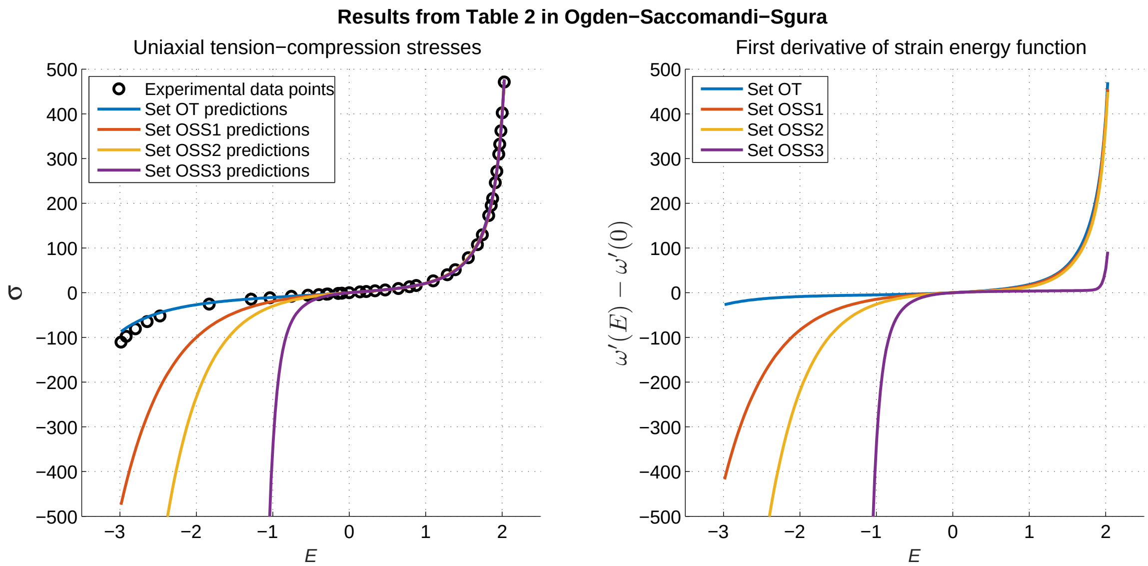

Figure 2: Left (a): Uniaxial tension-compression Cauchy stress predictions ($\mathrm{kg}\,/\,\mathrm{cm}^2$) computed by Ogden's model with $M = 4$ using parameter sets obtained by fitting uniaxial tension experimental data. Right (b): First derivative of the Ogden function term $\omega\,(E)$. Different curves correspond to the different parameter sets reported in Table 2 of Ogden et al. (2004).

of being determined from the actual material behavior, and the respective strain energy functions are very different to each other in the whole domain of deformations, not only in the tension domain, see Figure 4.b. Increasing the number of terms in Ogden's function may improve the fitting residuals within the corresponding domain, but it does not overcome the overall problem (Ogden et al., 2004).

Due to the very large discrepancies observed in the functions $\omega'\,(E)$ in Figures 3.b and 4.b, it should be evident that equibiaxial tension data only (equivalently, uniaxial compression data only) should never be used to determine an incompressible hyperelastic model at finite strains (cf. Kakavas (2000)), unless the uniaxial tension predictions are verified against experiments subsequently (Steinmann et al., 2012).

Finally, we show in Figure 5.a the uniaxial tension-compression predictions obtained by the Ogden model when the material parameters have been obtained fitting *simultaneously both* uniaxial *and* equibiaxial tension experimental data, i.e. the material parameters reported in Eqs. (32) and (33) (Section 4.4) of Reference Ogden et al. (2004). In this case, both solutions have been obtained from an experimental data set (the equivalent uniaxial tension-compression curve $\sigma_u\,(E)$) which is consistent with the underlying hypotheses of the model (isotropy, incompressibility

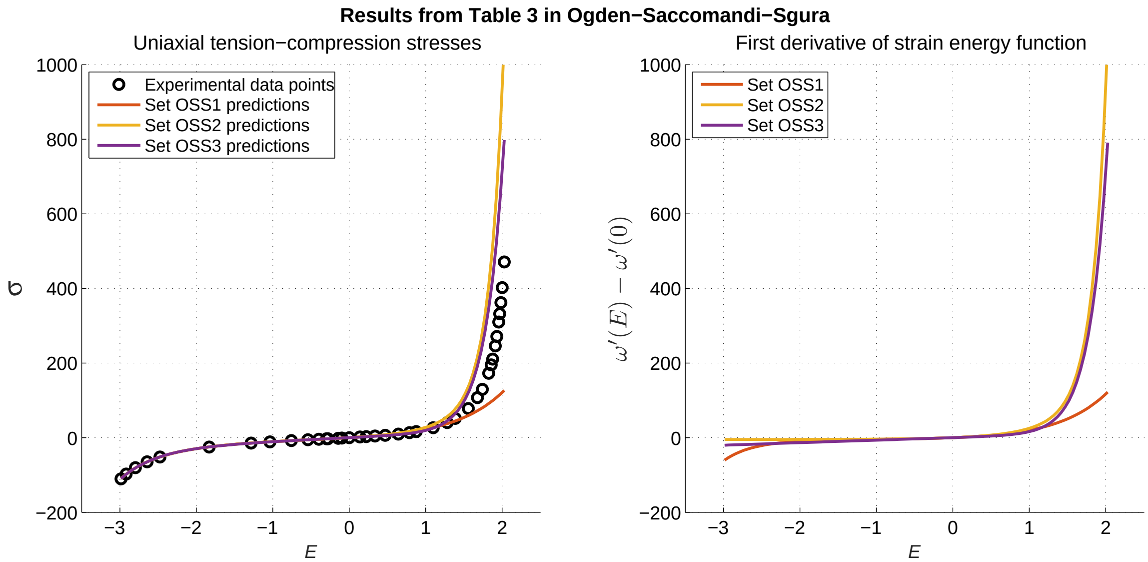

Figure 3: Left (a): Uniaxial tension-compression Cauchy stress predictions (kg / cm^2) computed by Ogden's model with $M = 3$ using parameter sets obtained by fitting equibiaxial tension experimental data. Right (b): First derivative of the Ogden function term $\omega(E)$. Different curves correspond to the different parameter sets reported in Table 3 of Ogden et al. (2004).

and the Valanis–Landel decomposition). The stress predictions in both cases are accurate and very similar to each other. Furthermore, the solution terms $\omega'(E)$ for $M = 3$ (Eq. (32) of Ogden et al. (2004)) and for $M = 4$ (Eq. (33) of Ogden et al. (2004)), even being slightly different, have the same tendency and are difficult to distinguish visually, see Figure 5.b. This explains why in this case the values of the solution parameters have remained the same for different starting values in the respective minimization problems. In this case, whether we use the model with $M = 3$ or with $M = 4$, we can ensure that the differences in the predictions in any generic multiaxial loading situation will be small and the required confidence in the numerical predictions will be attained even in the case of lack of unicity of material parameters. In fact, it can be observed in Figures 18 and 19 of Ogden et al. (2004) that the analytical stresses predicted in another boundary value problem are almost coincident if the parameters obtained this way are considered (compare both curves labelled as OSS^{se} in Figures 18 and 19 of Ogden et al. (2004)). Finally, note that now the conclusions raised in Ogden et al. (2004) regarding the (respective) fitting residuals associated to the other curves in Figures 18 and 19 of Ogden et al. (2004) are no longer relevant (recall the arbitrariness of $\omega'(E)$ in Figures 1.b, 2.b, 3.b and

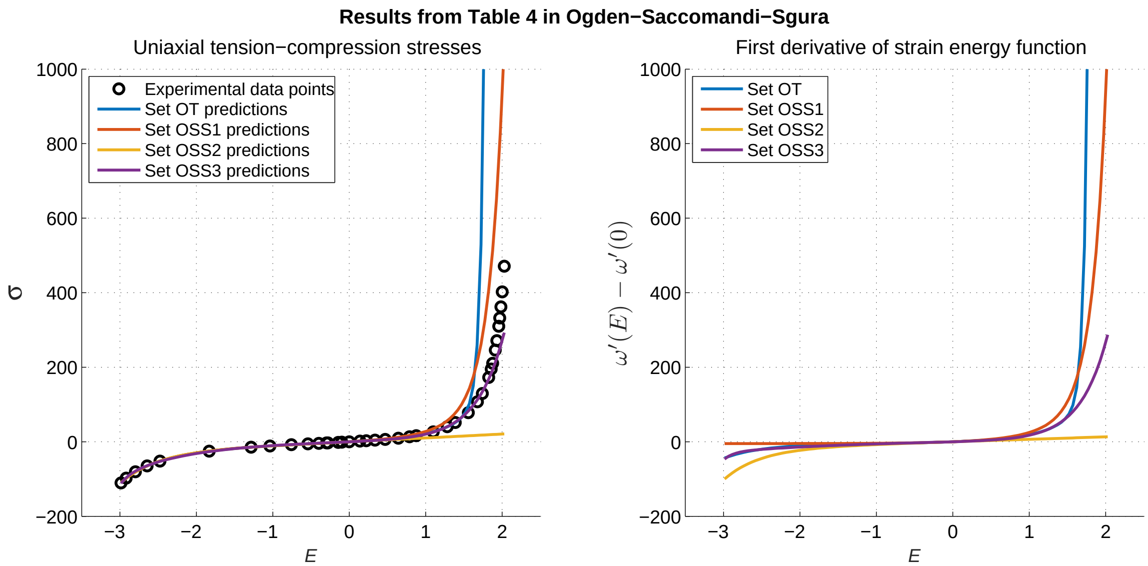

Figure 4: Left (a): Uniaxial tension-compression Cauchy stress predictions (kg / cm^2) computed by Ogden's model with $M = 4$ using parameter sets obtained by fitting equibiaxial tension experimental data. Right (b): First derivative of the Ogden function term $\omega(E)$. Different curves correspond to the different parameter sets reported in Table 4 of Ogden et al. (2004).

4.b).

5.2. Predictions using the Sussman–Bathe model

In this section we show the prediction capabilities of the Sussman–Bathe spline-based hyperelastic model. We explain and follow one possible well-posed procedure that uniquely determines this incompressible, isotropic model from experimental data. Even though this methodology differs from the usual approach (recall previous Sections), we bring recommendations of best practices for determining incompressible, isotropic hyperelastic models built on the basis of the Valanis–Landel hypothesis.

In the present incompressible, nonlinear case we need a complete tension-compression experimental data set, either $\sigma_u(E)$ or $\sigma_e(E)$, in order to be able to determine the first derivative function of the strain energy term $\omega(E)$ via the corresponding inversion formula solution; recall Eqs. (13) and (18). The inversion formulae are just making explicit the experimental data set that we need in order to find the solution to the problem at hand. If the compression branch of $\sigma_u(E)$, for example, is missing, then one must prescribe it before determining the strain energy function. This way the solution becomes unique and *one will get what one has prescribed.* This is the essence of the WYPIWYG philosophy (Sussman and Bathe, 2009; Latorre and Montáns, 2013,

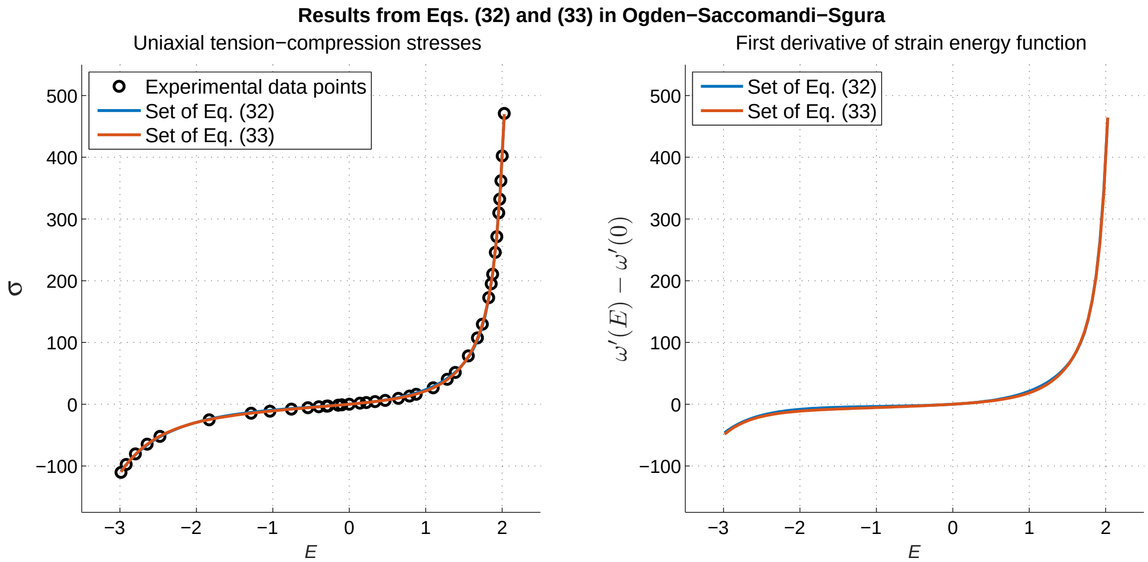

Figure 5: Left (a): Uniaxial tension-compression Cauchy stress predictions (kg / cm^2) computed by Ogden's model using parameter sets obtained by fitting simultaneously both uniaxial and equibiaxial tension experimental data. Right (b): First derivative of the Ogden function term $\omega(E)$. Different curves (almost indistinguishable) correspond to the different parameter sets reported in Eqs. (32) ($M = 3$) and (33) ($M = 4$) of Ogden et al. (2004).

2014; Latorre et al., 2016; Romero et al., 2017; Latorre and Montáns, 2015, 2016). If the uniaxial compression branch is unknown from experiments, a good option in some materials is to prescribe a symmetric stored energy function in the space of logarithmic strains (Moerman et al., 2016).

In Figure 6.a we represent the stress predictions obtained using the Sussman–Bathe model when two very different "experimental" tension-compression uniaxial data sets are prescribed. The "experimental" functions are separately obtained from the Ogden function with the solution set OSS_1 in Table 2 of Ogden et al. (2004) (computed from uniaxial tension data only) and the solution set OSS_2 in Table 4 of Ogden et al. (2004) (computed from equibiaxial tension data only), respectively. Note the very different uniaxial stress predictions that these parameter sets provide, even though both of them have been obtained in an attempt to describe the behavior of the same rubber-like material. The discrete point distributions in Figure 6.a represent the stresses predicted by the respective spline-based strain energy functions shown in Figure 6.b using Eq. (7). It can be seen that each model is capable of capturing exactly (up to numerical precision) the prescribed material behavior. In Figure 6.b we can also observe that we exactly retrieve the respective Ogden's function terms $\omega'(E)$ of Figures 2.b (set OSS_1) and 4.b (set OSS_2). Hence, this procedure provides a unique and meaningful solution for each material addressed, predicting adequately the behavior of the material in any other loading situation if the material really satisfies the preliminary assumptions.

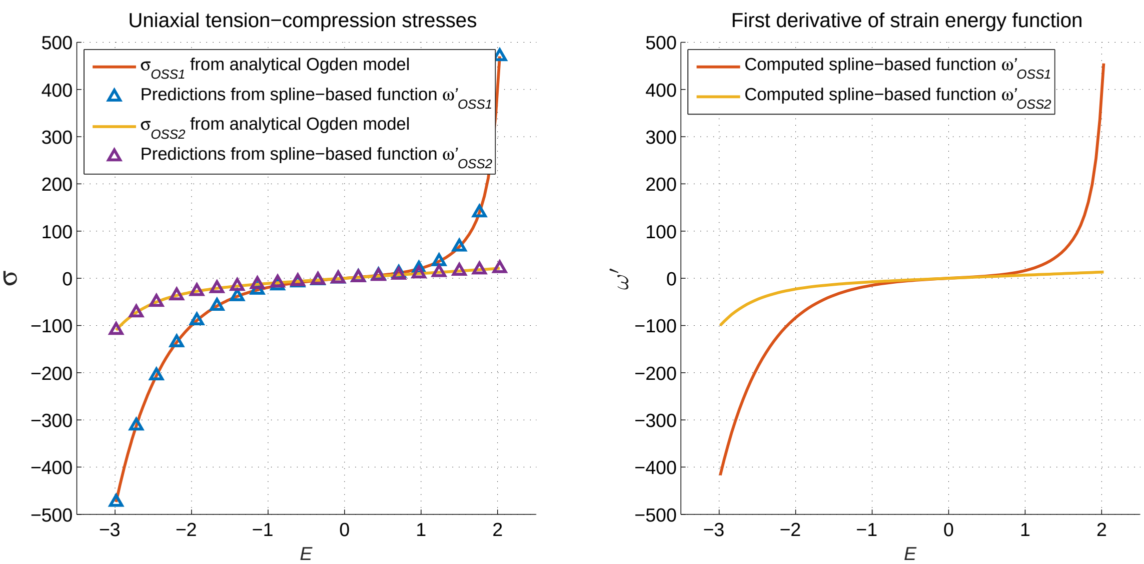

Figure 6: Left (a): Uniaxial tension-compression Cauchy stress predictions ($\mathrm{kg}\,/\,\mathrm{cm}^2$) of Ogden's model stresses obtained using the Sussman–Bathe model. Right (b): First derivative of the Sussman–Bathe function term $\omega(E)$. Different curves correspond to the parameter set OSS_1 in Table 2 of Ogden et al. (2004) and the parameter set OSS_2 in Table 4 of Ogden et al. (2004).

As we did in Figures 1.a to 5.a, we represent in Figure 7.a the equivalent uniaxial tension-compression experimental data of Treloar (1944) (hollow circles). We compute the spline-based solution function $\omega'(E)$ of Figure 7.b interpolating first the experimental data points using cubic splines (blue solid line of Figure 7.a), then applying the inversion formula of Eq. (14) at a new strain data set $\bar{\boldsymbol{E}}$ and subsequently interpolating the computed solution points $\bar{\boldsymbol{\omega}}'\left(\bar{\boldsymbol{E}}\right)$ (not represented in Figure 7.b). We finally represent in Figure 7.a the stresses predicted by the spline-based function $\omega'(E)$ of Figure 7.b using Eq. (7). Again, for a given interpolating function $\sigma_u(E)$ (blue solid line of Figure 7.a), the obtained solution for $\omega'(E)$ is unique and exact. It should not be surprising now that the Ogden model solutions of Figure 5.b (i.e. those obtained fitting simultaneously both uniaxial and equibiaxial tension tests) tend to the exact spline-based solution of Figure 7.b. This fact definitely shows that the Ogden model can be very accurate if it is properly determined, and in such case, the lack of unicity is quite irrelevant from a practical point of view.

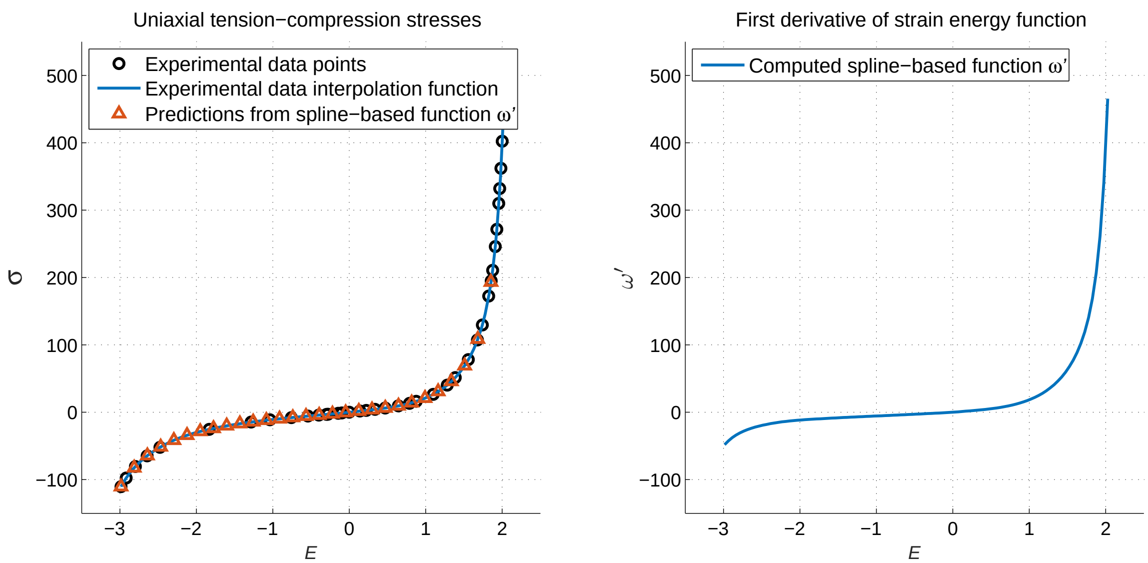

Figure 7: Left (a): Uniaxial tension-compression Cauchy stress predictions $(\mathrm{kg}\,/\,\mathrm{cm}^2)$ of Treloar's experimental data obtained using the Sussman–Bathe model. Right (b): First derivative of the Sussman–Bathe function term $\omega\,(E)$.

After determining the stored energy with a complete set of tests, we can verify the consistency of the basic assumptions included in the model by means of the comparison of the stresses predicted by the model with experimental data obtained in other tests, such as a pure shear test or biaxial tests. If these additional experimental data are not accurately predicted, then the only theoretical reason is that at least one of the hypotheses (incompressibility, isotropy, the Valanis–Landel form, etc.) is not adequate for the material being characterized. Then, a modification of the model formulation would be required. This is a relevant additional check for constitutive models.

We carry out this verification in Figure 8, where the pure shear stress function $\sigma_p\,(E) = \omega'\,(E) - \omega'\,(0) = \omega'\,(E)$ predicted by the spline-based term of Figure 7.b is compared to the experimental pure shear stress measurements of Treloar (1944). We can observe the very good agreement of the model predictions with the experimental data. This good agreement justifies the use of the hyperelastic, deviatoric model of Eq. (6) to characterize the mechanical behavior of the rubber-like material under study and makes feasible the use of the spline-based term of Figure 7.b to predict the material behavior under general loading situations and boundary conditions. Of course, the predictions obtained from the properly determined Ogden stored energies given in Fig. 5.b are almost identical to those shown in Figure 8. Remarkably, this specific model determination and verification procedure is also followed in Pancheri and Dorfmann (2014), where the authors emphasize "the importance of using multiple independent data sets to determine the magnitude of the parameters and to ensure a stable response over a wide range of deformations".

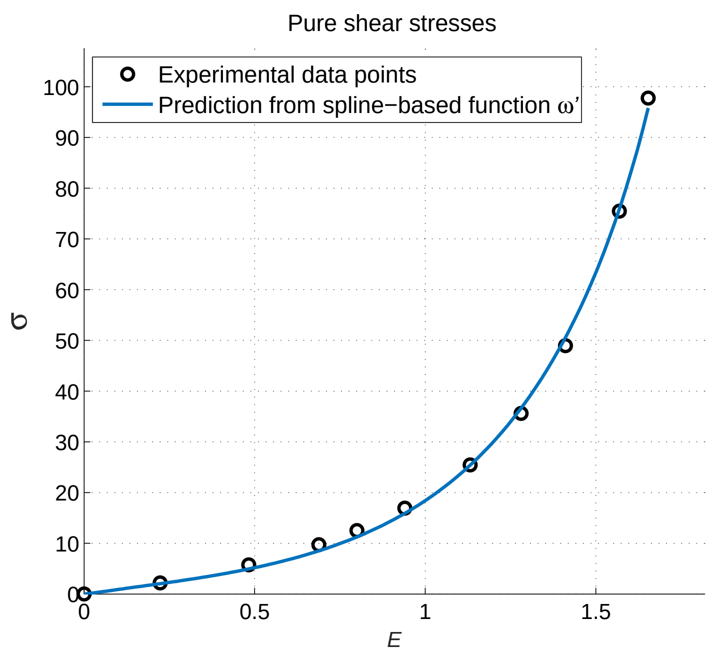

Figure 8: Pure shear Cauchy stress predictions (kg / cm^2) of Treloar's experiental data computed using the Sussman–Bathe function $\omega'(E)$ of Figure 7.b.

Finally, we note that many authors (Twizell and Ogden (1983); Maeda et al. (2015); Gendy and Saleeb (2000) to name a few) determine the assumed Valanis–Landel–type strain energy function solving optimization problems in which more than two test data sets are simultaneously fitted, e.g. uniaxial tension, equibiaxial tension and pure shear simultaneously. It can be deduced from the foregoing arguments that this problem is physically overdetermined. However, similarly to the underdetermined cases discussed above, this problem may still be solved due to the inherent nature of the least squares method, which in our opinion somehow hides the underlying physics again. Remarkably, we cannot proceed this way with the mathematically-exact, physically-based WYPIWYG method based on the inversion formula. However, this type of physically overdetermined procedures are better than the undetermined ones in the sense that they prevent the computation of arbitrary solutions, as those shown in Figures 1.b to 4.b, because the material information needed to determine $\omega(E)$ is included in the experimental data set considered. As explained in the Introduction Section, these facts seem to be not well understood in the literature, where both physically overdetermined and physically underdetermined procedures are indistinctly solved within the same work giving no clear justification for that.

6. Conclusion

In this paper we have theoretically addressed the adequate determination of the terms of stored energies. In order to present the concepts in a simple context we have used isotropic, incompressible materials following the Valanis-Landel decomposition. Even in this simplest case, frequent are the cases in the literature when an insufficient number of tests, the correct number of them or an excess of them are employed without a clear theoretical justification.

We have shown that, in general, both the extension *and* the compression branches of a uniaxial test are needed to completely characterize the material in order to use the resulting model in other loading situations with confidence in the results. In general, the use of only one branch of the tension-compression curve yields a physically underdetermined problem, whereas using more than the needed curves results in a physically overdetermined problem. This becomes apparent in the WYPIWYG approach because the exact solution is mathematically obtained, which in turn, clearly explains from a theoretical (physical) standpoint some of the empirical conclusions encountered in the literature. In our opinion, the use of material constants obtained only from tensile tests in general finite element simulations could be questioned, depending on how the material is working at the stress integration point. Then, our recommendations is that if the modeler does not have a complete set of experimental data defining the material behavior, a reasonable hypothesis based on engineering experience should be made for the missing parts *before* performing the determination of the material constants; or otherwise, the obtained behavior for that tests should be verified accordingly.

Acknowledgements

Partial financial support for this work has been given by grants DPI2011-26635 and DPI2015-69801-R from the Dirección General de Proyectos de Investigación of the Ministerio de Economía y Competitividad of Spain. Erica De Rosa acknowledges the funding for a stay at the UPM, Progetto di internazionalizzazione dei corsi di studio from COINOR-Università Degli Studi di Napoli Federico II. F.J. Montáns also acknowledges the support of the Department of Mechanical and Aerospace Engineering of University of Florida during the sabbatical period in which this paper was finished and that of Ministerio de Educación, Cultura y Deporte of Spain for the financial support for that stay under grant PRX15/00065.

References

Angeli, S., Panayiotou, C., Psimolophitis, E., Nicolaou, M., Constantinides, C., 2015. Uniaxial stress-strain characteristics of elastomeric membranes: Theoretical considerations, computational simulations, and experimental validation. Mechanics of Advanced Materials and Structures 22, 996–1006.

Ateshian, G., Warden, W., Kim, J., Grelsamer, R., Mow, V., 1997. Finite deformation biphasic material properties of bovine articular cartilage from confined compression experiments. Journal of Biomechanics 30, 1157–1164.

Barenblatt, G.I., Joseph, D.D., 2013. Collected Papers of RS Rivlin: Volume I and II. Springer Science & Business Media.

Bechir, H., Chevalier, L., Chaouche, M., Boufala, K., 2006. Hyperelastic constitutive model for rubber-like materials based on the first seth strain measures invariant. European Journal of Mechanics-A/Solids 25, 110–124.

Bradley, G., Chang, P., McKenna, G., 2001. Rubber modeling using uniaxial test data. Journal of Applied Polymer Science 81, 837–848.

Chen, H., Zhao, X., Lu, X., Kassab, G.S., 2016. Microstructure-based constitutive models for coronary artery adventitia, in: Structure-Based Mechanics of Tissues and Organs. Springer, pp. 225–248.

Chen, J., Ahmad, R., Li, W., Swain, M., Li, Q., 2015. Biomechanics of oral mucosa. Journal of The Royal Society Interface 12, 20150325.

Cooney, G.M., Moerman, K.M., Takaza, M., Winter, D.C., Simms, C.K., 2015. Uniaxial and biaxial mechanical properties of porcine linea alba. Journal of the Mechanical Behavior of Biomedical Materials 41, 68–82.

Cortes, D.H., Elliott, D.M., 2016. Modeling of collagenous tissues using distributed fiber orientations, in: Structure-Based Mechanics of Tissues and Organs. Springer, pp. 15–39.

Destrade, M., Dorfmann, L., 2015. Ray W Ogden: An appreciation. Mathematics and Mechanics of Solids 20, 621–624.

Fehervary, H., Smoljkić, M., Vander Sloten, J., Famaey, N., 2016. Planar biaxial testing of soft biological tissue using rakes: a critical analysis of protocol and fitting process. Journal of the Mechanical Behavior of Biomedical Materials 61, 135–151.

Fung, Y.C., 2013. Biomechanics: Mechanical Properties of Living Tissues. Springer, New York.

Gasser, T.C., 2016. Histomechanical modeling of the wall of abdominal aortic aneurysm, in: Structure-Based Mechanics of Tissues and Organs. Springer, pp. 57–78.

Gendy, A., Saleeb, A., 2000. Nonlinear material parameter estimation for characterizing hyper elastic large strain models. Computational Mechanics 25, 66–77.

Grytz, R., Meschke, G., Jonas, J.B., Downs, J.C., 2016. Glaucoma and structure-based mechanics of the lamina cribrosa at multiple scales, in: Structure-Based Mechanics of Tissues and Organs. Springer, pp. 93–122.

Hariharaputhiran, H., Saravanan, U., 2016. A new set of biaxial and uniaxial experiments on vulcanized rubber and attempts at modeling it using classical hyperelastic models. Mechanics of Materials 92, 211–222.

Holzapfel, G.A., 2000. Nonlinear Solid Mechanics. Wiley, Chichester.

Holzapfel, G.A., 2006. Determination of material models for arterial walls from uniaxial extension tests and histological structure. Journal of Theoretical Biology 238, 290–302.

Holzapfel, G.A., Niestrawska, J.A., Ogden, R.W., Reinisch, A.J., Schriefl, A.J., 2015. Modelling non-symmetric collagen fibre dispersion in arterial walls. Journal of The Royal Society Interface 12, 20150188.

Humphrey, J.D., 2013. Cardiovascular Solid Mechanics: Cells, Tissues, and Organs. Springer, New York.

Itskov, M., Aksel, N., 2004. A class of orthotropic and transversely isotropic hyperelastic constitutive models based on a polyconvex strain energy function. International Journal of Solids and Structures 41, 3833–3848.

Kakavas, P., 2000. A new development of the strain energy function for hyperelastic materials using a logarithmic strain approach. Journal of Applied Polymer Science 77, 660–672.

Kamenskiy, A.V., Pipinos, I.I., Dzenis, Y.A., Phillips, N.Y., Desyatova, A.S., Kitson, J., Bowen, R., MacTaggart, J.N., 2015. Effects of age on the physiological and mechanical characteristics of human femoropopliteal arteries. Acta Biomaterialia 11, 304–313.

Kearsley, E., Zapas, L., 1980. Some methods of measurement of an elastic strain-energy function of the valanis-landel type. Journal of Rheology (1978-present) 24, 483–500.

Khajehsaeid, H., Arghavani, J., Naghdabadi, R., 2013. A hyperelastic constitutive model for rubber-like materials. European Journal of Mechanics-A/Solids 38, 144–151.

Latorre, M., Montáns, F.J., 2013. Extension of the Sussman–Bathe spline-based hyperelastic model to incompressible transversely isotropic materials. Computers & Structures 122, 13–26.

Latorre, M., Montáns, F.J., 2014. What-You-Prescribe-Is-What-You-Get orthotropic hyperelasticity. Computational Mechanics 53, 1279–1298.

Latorre, M., Montáns, F.J., 2015. Anisotropic finite strain viscoelasticity based on the sidoroff multiplicative decomposition and logarithmic strains. Computational Mechanics 56, 503–531.

Latorre, M., Montáns, F.J., 2015. Material-symmetries congruency in transversely isotropic and orthotropic hyperelastic materials. European Journal of Mechanics-A/Solids 53, 99–106.

Latorre, M., Montáns, F.J., 2016. Fully anisotropic finite strain viscoelasticity based on a reverse multiplicative decomposition and logarithmic strains. Computers & Structures 163, 56–70.

Latorre, M., Romero, X., Montáns, F.J., 2016. The relevance of transverse deformation effects in modeling soft biological tissues. International Journal of Solids and Structures 99, 57–70.

Lee, L.C., Wenk, J., Klepach, D., Kassab, G.S., Guccione, J.M., 2016. Structural-based models of ventricular myocardium, in: Structure-Based Mechanics of Tissues and Organs. Springer, pp. 249–263.

Li, D., Robertson, A.M., 2009. A structural multi-mechanism constitutive equation for cerebral arterial tissue. International Journal of Solids and Structures 46, 2920–2928.

Lopez-Pamies, O., 2010. A new I_1-based hyperelastic model for rubber elastic materials. Comptes Rendus Mecanique 338, 3–11.

Maeda, N., Fujikawa, M., Makabe, C., Yamabe, J., Kodama, Y., Koishi, M., 2015. Performance evaluation of various hyperelastic constitutive models of rubbers. Constitutive Models for Rubber IX , 271.

Mansouri, M., Darijani, H., 2014. Constitutive modeling of isotropic hyperelastic materials in an exponential framework using a self-contained approach. International Journal of Solids and Structures 51, 4316–4326.

Marckmann, G., Verron, E., 2006. Comparison of hyperelastic models for rubber-like materials. Rubber Chemistry and Technology 79, 835–858.

Moerman, K.M., Simms, C.K., Nagel, T., 2016. Control of tension–compression asymmetry in Ogden hyperelasticity with application to soft tissue modelling. Journal of the Mechanical Behavior of Biomedical Materials 56, 218–228.

Natali, A.N., Carniel, E.L., Pavan, P.G., Dario, P., Izzo, I., 2006. Hyperelastic models for the analysis of soft tissue mechanics: definition of constitutive parameters, in: The First IEEE/RAS-EMBS International Conference on Biomedical Robotics and Biomechatronics, 2006. BioRob 2006., IEEE. pp. 188–191.

Ogden, R., Saccomandi, G., Sgura, I., 2004. Fitting hyperelastic models to experimental data. Computational Mechanics 34, 484–502.

Ogden, R.W., 1997. Non-linear Elastic Deformations. Dover, New York.

Ogden, R.W., 2004. Mechanics and Thermomechanics of Rubberlike Solids. Springer, Wien. volume 452 of *CISM courses and lectures Series*. chapter Elasticity and inelasticity of rubber. pp. 135–185.

Palmieri, G., Sasso, M., Chiappini, G., Amodio, D., 2009. Mullins effect characterization of elastomers by multi-axial cyclic tests and optical experimental methods. Mechanics of Materials 41, 1059–1067.

Pancheri, F.Q., Dorfmann, L., 2014. Strain-controlled biaxial tension of natural rubber: new experimental data. Rubber Chemistry and Technology 87, 120–138.

Pierce, D.M., Maier, F., Weisbecker, H., Viertler, C., Verbrugghe, P., Famaey, N., Fourneau, I., Herijgers, P., Holzapfel, G.A., 2015. Human thoracic and abdominal aortic aneurysmal tissues: damage experiments, statistical analysis and constitutive modeling. Journal of the Mechanical Behavior of Biomedical Materials 41, 92–107.

Puglisi, G., Saccomandi, G., 2016. Multi-scale modelling of rubber-like materials and soft tissues: an appraisal, in: Proc. R. Soc. A, The Royal Society. p. 20160060.

Rivlin, R.S., Saunders, D., 1951. Large elastic deformations of isotropic materials. vii. experiments on the deformation of rubber. Philosophical Transactions of the Royal Society of London A: Mathematical, Physical and Engineering Sciences 243, 251–288.

Romero, X., Latorre, M., Montáns, F., 2017. Determination of the WYPIWYG strain energy density of skin through finite element analysis of the experiments on circular specimens. Under Review .

Sacks, M.S., 2003. Incorporation of experimentally-derived fiber orientation into a structural constitutive model for planar collagenous tissues. Journal of Biomechanical Engineering 125, 280–287.

Santamaría, V.A., Siret, O., Badel, P., Guerin, G., Novacek, V., Turquier, F., Avril, S., 2015. Material model calibration from planar tension tests on porcine linea alba. Journal of the Mechanical Behavior of Biomedical Materials 43, 26–34.

Shearer, T., 2015. A new strain energy function for the hyperelastic modelling of ligaments and tendons based on fascicle microstructure. Journal of Biomechanics 48, 290–297.

Steinmann, P., Hossain, M., Possart, G., 2012. Hyperelastic models for rubber-like materials: consistent tangent operators and suitability for treloars data. Archive of Applied Mechanics 82, 1183–1217.

Stumpf, F., Marczak, R., 2010. Optimization of constitutive parameters for hyperelastic models satisfying the baker-ericksen inequalities. Mecánica Computacional 29, 2901–2916.

Sussman, T., Bathe, K.J., 2009. A model of incompressible isotropic hyperelastic material behavior using spline interpolations of tension–compression test data. Communications in Numerical Methods in Engineering 25, 53–63.

Treloar, L., 1944. Stress-strain data for vulcanised rubber under various types of deformation. Transactions of the Faraday Society 40, 59–70.

Treloar, L.R.G., 1975. The physics of rubber elasticity. Oxford University Press, Oxford.

Tricerri, P., Dedè, L., Gambaruto, A., Quarteroni, A., Sequeira, A., 2016. A numerical study of isotropic and anisotropic constitutive models with relevance to healthy and unhealthy cerebral arterial tissues. International Journal of Engineering Science 101, 126–155.

Twizell, E., Ogden, R., 1983. Non-linear optimization of the material constants in ogden's stress-deformation function for incompressinle isotropic elastic materials. The Journal of the Australian Mathematical Society. Series B. Applied Mathematics 24, 424–434.

Urayama, K., 2006. An experimentalist's view of the physics of rubber elasticity. Journal of Polymer Science Part B: Polymer Physics 44, 3440–3444.

Valanis, K., Landel, R., 1967. The strain-energy function of a hyperelastic material in terms of the extension ratios. Journal of Applied Physics 38, 2997–3002.

Van Loocke, M., Lyons, C., Simms, C., 2006. A validated model of passive muscle in compression. Journal of Biomechanics 39, 2999–3009.